7070 Inorg. Chem. 2009, 48, 7070–7079
DOI: 10.1021/ic801794e

Inorganic Chemistry
Article

Apical Ligand Substitution, Shape Recognition, Vapor-Adsorption Phenomenon, and Microcalorimetry for a Pillared Bilayer Porous Framework That Shrinks or Expands in Crystal-to-Crystal Manners upon Change in the Cobalt(II) Coordination Environment

Ming-Hua Zeng,*,† Sheng Hu,‡ Qing Chen,† Gang Xie,§ Qi Shuai,§ Sheng-Li Gao,§ and Li-Yuan Tang∥

†*Key Laboratory for the Chemistry and Molecular Engineering of Medicinal Resources (Ministry of Education of China), School of Chemistry & Chemical Engineering of Guangxi Normal University, Guilin 541004, P. R. China,* ‡*Faculty of Chemical Engineering and Light Industry, Guangdong University of Technology, Guangzhou 510006, P. R. China,* §*Department of Chemistry, Northwest University, Xi'an 710069, P. R. China, and* ∥*Key Laboratory for Polymeric Composite and Functional Materials of Ministry of Education, Guangzhou 510275, P. R. China*

Received September 19, 2008

A 2D pillared bilayer coordination polymer, $[Co(5\text{-}NH_2\text{-}bdc)(bpy)_{0.5}(H_2O)]\cdot 2H_2O$ (**1**; 5-NH_2-bdc = 5-aminoisophthalate; bpy = 4,4′-bipyridine) has been hydrothermally synthesized and shows a novel microporous host framework with 1D channels and high thermal stability (~400 °C). The framework of **1** exhibits reversible single-crystal-to-single-crystal transformations upon removing and rebinding the coordinated waters as well as replacing them with MeOH and EtOH from the solvent. X-ray crystallography reveals that the coordination geometry of Co(II) changes from octahedron to square pyramid, as well as the shrinkage/expansion of pore deformation in respect to the subsequent shear motion of bpy pillars and vice versa. The dehydrated form **2** exhibits a shape recognition ability, which can accommodate linear molecules, such as MeCN and 2-propynyl alcohol, and interesting storage capabilities for oversized MeOH, EtOH, and benzene molecules, concomitant with spongelike dynamic transformation. The microcalorimetric study indicates that the crystalline state−liquid guest exchange and guest inclusion processes (**1** ⊃ MeOH or EtOH, **2** ⊃ MeOH, EtOH or MeCN) are feasibly endothermic reactions with the values of molar enthalpy, ΔH^{θ}_{m}, of +21.38(96), +12.68(85), +25.92(86), +17.03(57), and +14.93(75) kJ mol^{-1}, respectively.

Introduction

The rapid development of microporous metal-organic frameworks (MOFs) has led to an active discussion of these materials with high prospects for practical applications.[1,2] In particular, flexible MOF materials retain crystallinity after some structural transformations, including shrinking or expanding in response to external stimuli, which is essentially distinct from that of the rigid classical porous materials.[3] Those dynamic single-crystal-to-single-crystal (SCSC) transformations are induced by the removal and readsorption of guest molecules or caused by the removal or addition of ligands from or to the host framework itself, which further means the probable incorporation of coordinatively unsaturated metal centers (UMCs) into a porous host. Obviously, the above transformations have been anticipated to show high selectivity, accommodation, and separation of specific molecules, which may also be directly visualized by crystallographic analysis.[4,5] In fact, designing the guest-responsive pores of flexible MOFs that are accompanied by significant atomic motions and obvious changes in the framework has

*To whom correspondence should be addressed. E-mail: zmh@mailbox.gxnu.edu.cn. Fax: 86 773 2120-958.

(1) (a) James, S. L. *Chem. Soc. Rev.* **2003**, *32*, 276 and references therein. (b) Yaghi, O. M.; O'Keeffe, M.; Ockwig, N. W.; Chae, H. K.; Eddaoudi, M.; Kim, J. *Nature* **2003**, *423*, 705. (c) Rosi, N. L.; Eckert, J.; Eddaoudi, M.; Vodak, D. T.; Kim, J.; O'Keeffe, M.; Yaghi, O. M. *Science* **2003**, *300*, 1127. (d) Kitagawa, S.; Kitaura, R.; Noro, S. *Angew. Chem., Int. Ed.* **2004**, *43*, 2334. (e) El-Kaderi, H. M.; Hunt, J. R.; Mendoza-Cortés, J.; Cté, A. P.; Taylor, R. E.; O'Keeffe, M.; Yaghi, O. M. *Science* **2007**, *316*, 1268. (f) Serre, C.; Mellot-Draznieks, C.; Surblé, S.; Audebrand, N.; Filinchuk, Y.; Férey, G. *Science* **2007**, *315*, 1828.
(2) (a) Maspoch, D.; Ruiz-Molina, D.; Veciana, J. *Chem. Soc. Rev.* **2007**, *36*, 770. (b) Mueller, U.; Schubert, F. M.; Puetter, H.; Teich, K.; Schierle-Arndt, Pastré, J. *J. Mater. Chem.* **2006**, *16*, 626. (c) Kepert, C. J. *Chem. Commun.* **2006**, 695. (d) Ouellette, W.; Prosvirin, A. V.; Whitenack, K.; Dunbar, K. R.; Zubieta, J. **2009**. *48*, 2140.
(3) (a) Kitagawa, S.; Uemura, K. *Chem. Soc. Rev.* **2005**, *34*, 109 and references therein. (b) Kitagawa, S.; Matsuda, R. *Coord. Chem. Rev.* **2007**, *251*, 2490.
(4) Kawano, M.; Fujita, M. *Coord. Chem. Rev.* **2007**, *251*, 2592.
(5) (a) Suh, M. P.; Cheon, Y. E. *Aust. J. Chem.* **2006**, *59*, 605. (b) Halder, G. J.; Kepert, C. J. *Aust. J. Chem.* **2006**, *59*, 597. (c) Zheng, S.-L.; Vande Velde, C. M. L.; Messerschmidet, M.; Volkov, A.; Gembicky, M.; Coppens, P. *Chem.—Eur. J.* **2008**, *14*, 706.

 Published on Web 07/09/2009

Scheme 1. (a) Summary of the Crystalline-State Ligand Exchange and Guest Inclusion and (b) Summary of the Variety of Cell Volumes upon SCSC Transformation

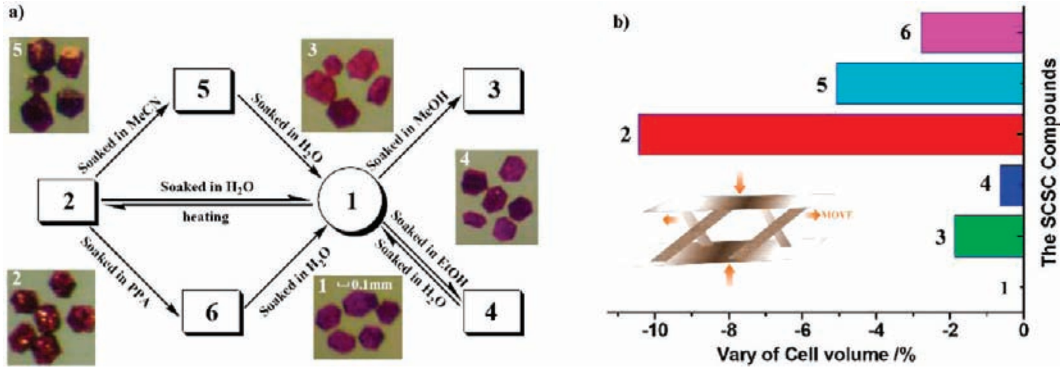

recently become a new state-of-the-art field. However, a few MOFs are stable upon thermal liberation of volatile coordinated ligands. It is still a challenge to successfully immobilize UMCs onto the MOF pores to exhibit SCSC transformation as well as decorate the apertures on size or chemical characteristics upon the change in the metal coordination environment.[4−6] On the other hand, as a kind of important potential porous material with special structures, the thermodynamic properties of MOFs and their SCSC transformations with crystalline-state guest exchange and inclusion are helpful to better understand and explain molecular interactions, especially to test and develop new models and theories that are able to describe the thermodynamic behavior of solid or crystalline state−liquid reactions and interactions, which are obviously more complicated than the solid state−gas adsorption process.[7] In addition to the single-crystal X-ray diffraction method exhibiting powerful help in the study of reversibly dynamic structural changes, the microcalorimetric method may provide another effective technique for exploring the dynamic host−guest chemistry of coordination frameworks under crystalline state−liquid reactions and interactions.[8]

Our previous works show that a judicious choice of the appropriate secondary building units and linear and rigid bifunctional ligands as the spacers may enable an observation of dynamic transformations of porous materials.[9] In particular, the "pillared-layer" motif is a good candidate for such materials because the pillars can act as dynamic components in MOFs.[3,10] Among them, stable pillared bilayer frameworks that contain proper, unoccupied voids, as intermediates between the 3D and low dimensional systems, are good

Scheme 2. The Enthalpies of Reaction of Different Crystalline-State Ligand Substitutions and Guest Exchange/Inclusion Processing

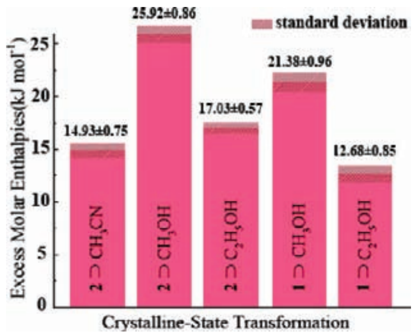

models for studying SCSC transformations.[3−5] Cobalt(II) is a potential UMC because it can adopt diverse coordination environments. It is also a classical example that shows chromism upon ligand exchange or removal in the solid state.[6] The ligand-exchange process has been seldom observed by single-crystal X-ray diffraction studies, especially for several different solvent ligand exchanges in the same MOF, because the drastic structural changes can cause single crystals of MOFs to break into small pieces and lose transparency. Following the above considerations, we report a novel flexible porous 2D pillared bilayer coordination polymer, namely, [Co(5-NH$_2$-bdc)(bpy)$_{0.5}$(H$_2$O)]·2H$_2$O (**1**) (5-NH$_2$-bdc = 5-aminoisophthalate, bpy = 4,4′-bipyridine), which has been characterized by single-crystal X-ray diffraction in a variety of different SCSC transformation forms and molar enthalpies of the crystalline-state guest exchange and inclusion reaction processes (Schemes 1 and 2). As will be shown, a flexible pillared bilayer framework is effectively controlled by the shear motion of pillars, followed by the departure of aqua ligands or the addition of new terminal ligands to the UMCs.

Experimental Section

Materials and Physical Measurements. The reagents and solvents employed were commercially available and used as received without further purification. C, H, and N microanalyses were carried out with an Elementar Vario-EL CHNS elemental analyzer. The FT-IR spectra were recorded from KBr pellets in the range 4000−400 cm^{-1} on a Bio-Rad FTS-7 spectrometer. X-ray powder diffraction (XRPD) intensities were measured when heated from 25 to 650 °C on a Rigaku D/max-IIIA diffratometer (Cu Kα, λ = 1.54056 Å). The crystalline powder samples were prepared by crushing the single

(6) (a) Chen, C.-L.; Goforth, A. M.; Smith, M. D.; Su, C.-Y.; zur Loye, H.-C. *Angew. Chem., Int. Ed.* **2005**, *44*, 6673. (b) Takaoka, K.; Kawano, M.; Tominaga, M.; Fujita, M. *Angew. Chem., Int. Ed.* **2005**, *44*, 2151.
(7) Haneda, T.; Kawano, M.; Kawamichi, T.; Fujita, M. *J. Am. Chem. Soc.* **2008**, *130*, 1578.
(8) (a) Fischer, S.; Krahn, G.; Reimer, B. *Thermochim. Acta* **2006**, *445*, 160. (b) Wan, P.; Tong, H.; Zhua, Z.-H.; Shen, X.-Y.; Yan, J.; Hua, J.-M. *Mater. Sci. Eng., A* **2007**, *458*, 244. (c) Quaschning, V.; Auroux, A.; Deutsch, J.; Lieske, H.; Kemnitz, E. *J. Catal.* **2001**, *203*, 426. (d) Belkhadem, F.; Maldonado, A.; Siebenhaar, B.; Clacens, J.-M.; Perez Zurita, M. J.; Bengueddach, A.; Figueras, F. *Appl. Clay Sci.* **2008**, *39*, 28.
(9) (a) Hu, S.; He, K.-H.; Zeng, M.-H.; Zou, H.-H.; Jiang, Y.-M. *Inorg. Chem.* **2008**, *47*, 5218. (b) Hu, S.; Zhang, J.-P.; Li, H.-X.; Tong, M.-L.; Chen, X.-M.; Kitagawa, S. *Cryst. Growth. Des.* **2007**, 2286. (c) Zeng, M.-H.; Feng, X.-L.; Chen, X.-M. *Dalton Trans.* **2004**, 2217.
(10) (a) Takaoka, K.; Kawano, M.; Tominaga, M.; Fujita, M. *Angew. Chem., Int. Ed.* **2005**, *44*, 2151. (b) Zeng, M.-H.; Feng, X.-L.; Zhang, W.-X.; Chen, X.-M. *Dalton Trans.* **2006**, 5294. (c) Zeng, M.-H.; Gao, S.; Yu, X.-L.; Chen, X.-M. *New. J. Chem.* **2003**, *27*, 1599.

crystals and scanned from 3 to 65° with a step of 0.1°/s. The calculated patterns of **1** were generated with PowderCell. The sorption isotherms for methanol, ethanol, and benzene vapors were measured with an automatic gravimetric adsorption apparatus (IGA-003 series, Hiden Isochema Ltd.) at 298 K. The as-synthesized samples (weight 50−100 mg) were placed in a quartz tube and dried under a high vacuum at 393 K for 12 h to remove the solvent molecules prior to measurements. All of the starting materials employed were analyzed by a gravimetric analyzer (Pyris Diamond TG/DTA) heated from 20 to 150 or 900 °C with a rate of 10 °C/min. The calorimetric experiment was performed by using a RD496-III type microcalorimeter.[11] The calorimetric constants at 295.15, 298.15, 301.15, 304.15, and 307.15 K were determined, by the Joule effect, to be 63.799 ± 0.025, 63.901 ± 0.030, 64.000 ± 0.026, 64.075 ± 0.038, and 64.203 ± 0.043 μV/mW, respectively. The enthalpy of the dissolution of KCl (spectral purity) in deionized water was measured to be 17.238 ± 0.048 kJ/mol, which is in good agreement with the value of 17.241 ± 0.018 kJ/mol from ref 12. The accuracy is 0.02%, and the precision is 0.3%, which indicates that the calorimetric system is accurate and reliable. The reaction solvent (1 mL) was put into a stainless steel sample cell in a 15 mL container.[13] At equilibrium, the containers of the single crystal samples (8−10 mg; crystal average size, 3.0−6.0 × 10^{-3} mm^3) were pushed down simultaneously. As a result, the crystal solvent was mixed at 298.15 K, and the thermogram of the crystalline-state−liquid guest exchange and guest inclusion was recorded.

Syntheses. Preparation of 1. A mixture of $Co(NO_3)_2 \cdot 6H_2O$ (0.298 g, 1.0 mmol), NaOH (0.080 g, 2.0 mmol), 5-aminoisophthalate (0.316 g, 1.0 mmol), 4,4′-bipyridine (0.156 g, 1.0 mmol), and H_2O (15.0 mL) was stirred for 20 min in the air. Then, the mixture was placed in a 23 mL Teflon-lined autoclave and heated at 130 °C for 72 h. The autoclave was cooled over a period of 16 h at a rate of 5 °C h^{-1}, and **1**, as black-red block crystals, was collected by filtration, washed with water, and dried at ambient temperature. Yield: 60% (based on Co). Elem Anal. Calcd for **1**, $C_{13}H_{15}CoN_2O_7$ (370.20) (%): C, 42.18; H, 4.08; N, 7.57. Found (%): C, 42.12; H, 4.10; N, 7.55. IR for **1** (KBr, cm^{-1}): 3352s, 3278vs, 3169s, 1612s, 1560vs, 1541vs, 1483w, 1444m, 1381vs, 1330m, 1074m, 972w, 799w, 778m, 726m, 638w, 519w.

Preparation of 2. Anhydrous **2** was obtained by heating crystals of **1** under a vacuum at 120 °C for 2 h. Although some crystals were cracked, the others retained their primary well-defined external shapes after the heating process.

Preparations of 3, 4, 5, and 6. After immersing proper-size crystals of **1** in a MeOH or EtOH solvent in small sealed tubes, separately, at room temperature for one day, the crystals retained their primary well-defined external forms, with the microporous space of the crystals accommodating new guest molecules, which were stable in the atmosphere. To further check the oversized guest molecules' inclusion properties of **2** and examine whether the framework could be reversible, a crystalline sample of **2** was immersed in a variety of wet solvents (MeCN, PPA). Elem Anal. Calcd for **3**, $C_{14}H_{15}CoN_2O_6$ (366.21) (%): C, 45.92; H, 4.13; N, 7.65. Found (%): C, 45.82; H, 4.20; N, 7.60. Calcd for **4**, $C_{15}H_{17}CoN_2O_6$ (380.24) (%): C, 47.38; H, 4.51; N, 7.37. Found (%): C, 47.35; H, 4.59; N, 7.36. Calcd for **5**, $C_{15}H_{12}CoN_3O_4$ (357.21) (%): C, 50.44; H, 3.39; N, 11.76. Found (%): C, 50.42; H, 3.47; N, 11.67. Calcd for **6**, $C_{16}H_{13}CoN_2O_5$ (372.22) (%): C, 51.63; H, 3.52; N, 7.53. Found (%): C, 51.60; H, 3.59; N, 7.47. The IR spectrum of **3** shows absorptions at 2948m and 2832m cm^{-1}, which can be attributed to the characteristic vibrations of MeOH, while that of **4** shows absorptions at 2974m and 2901m cm^{-1}, which can be attributed to the characteristic vibrations of EtOH. In the spectrum of **5**, the absorptions at 2963m and 2934m cm^{-1} are attributed to the characteristic vibrations of MeCN, and **6** shows absorptions at 2929w, 2873w, and 2120w cm^{-1}, which can be attributed to the characteristic vibrations of PPA.

Rehydration of 2−6. Standing the tested single-crystal sample of **2** in the air (T = 22(2) °C, relative humidity = 35(5)%) for several days gave rise to the rehydrated **1′**. The transformed single-crystal samples (**3**−**6**) were briefly immersed into water at room temperature for 1−2 h to achieve rehydration.

X-Ray Crystallography. Diffraction intensities of all compounds were collected on a Bruker Apex CCD area-detector diffractometer (Mo Kα, λ = 0.71073 Å). Absorption corrections were applied by the using multiscan program SADABS.[14] The structures were solved with direct methods and refined with a full-matrix least-squares technique with the SHELXTL program package.[15] All non-hydrogen atoms were refined with anisotropic displacement parameters, except parts of disordered solvent molecules of **1**, **4h**, and **6**. For all structures, the refinements revealed 2-fold disorder of bpy, and the solvent molecules in the above compounds were disordered and located from difference maps. The organic hydrogen atoms were generated geometrically (C−H, 0.96 Å); the aqua hydrogen atoms were located from difference maps and refined with isotropic temperature factors. The disorder was treated by performing half-occupancies with C and O atoms of the guest molecules of **6**. Crystal data as well as details of data collection and refinements for all complexes are summarized in Table 1 and Table S1 (Supporting Information). Selected bond distances and bond angles are listed in Table 2 and Tables S2 and S3 (Supporting Information). CCDC numbers 693810−693814, for **1** and **1′** to **1′′′′** and 693815−693821 for **2**, **3**, **3h**, **4**, **4h**, **5**, and **6**, respectively, contain the supplementary crystallographic data for this paper. These data can be obtained free of charge via www.ccdc.can.ac.uk/conts/retrieving.html (or from the Cambridge Crystallographic Centre, 12 Union Road, Cambridge CB21EZ, U.K.; fax: (+44)1223−336−033; e-mail: deposit@ccdc.cam.ac.uk).

Results and Discussion

Crystal Structures. The crystal structure of **1** is constructed from 2D thin layers interlinked through bridging bpy ligands into an interesting pillared bilayer framework. In **1** (Figure 1a), each octahedral Co(II) is coordinated with three different 5-NH_2-bdc ligands, one bpy ligand, and one terminal aqua ligand [$Co-O_{water}$ = 2.244(4) Å]. Each 5-NH_2-bdc ligand binds three Co(II) atoms [Co···Co separations of 7.686(1)−8.891(1) Å] through one amino group and one monodentate and one chelated carboxylate group in a triangular topology. This results in a neutral and essentially planar infinite 2D $[Co(5\text{-}NH_2\text{-}bdc)(H_2O)]_n$ layer with (6,3) topology where all terminal aqua ligands are oriented on the same side of the layer (Figure 1b). The bpy ligands act as pillars to link a pair of such layers and create 1D channels inside the bilayers. The 1D channels run along the b axis with dimensions of 3.2 × 6.2 $Å^2$ (taking account of the van der Waals radii), as calculated by the spaces between the H atoms of the terminal aqua ligand and the aromatic C−H groups of bpy, respectively. There are three water molecules per formula unit, determined by X-ray single-crystal diffraction analysis and further examined by thermalgravimetric analysis (TG), which are located within these channels and involved in extensive hydrogen-bonding interactions with the framework (Figure 2a, top).

(11) Ji, M.; Liu, M.-Y.; Gao, S.-L. *Instrum. Sci. Technol.* **2001**, *29*, 53.
(12) Marthada, V. K. *J. Res. NBS Standards* **1980**, *85*, 467.
(13) Gao, S.-L.; Fang, Y.; Chen, S.-P. *Acta Chim. Sin.* **2002**, *60*, 2220.
(14) Sheldrick, G. M. *SADABS 2.05*; University of Göttingen: Göttingen, Germany.
(15) *SHELXTL 6.10*; Bruker Analytical Instrumentation: Madison, WI, 2000.

Table 1. Crystal Data and Structure Refinement for **1**−**6** and **4h**

compound	1	2	3	4	4h	5	6
formula	$C_{13}H_{15}CoN_2O_7$	$C_{13}H_9CoN_2O_4$	$C_{14}H_{15}CoN_2O_6$	$C_{15}H_{17}CoN_2O_6$	$C_{15}H_{17}CoN_2O_6$	$C_{15}H_{12}CoN_3O_4$	$C_{16}H_{13}CoN_2O_5$
fw	370.20	316.15	366.21	380.24	380.24	357.21	316.15
temp/K	293(2)	293(2)	173(2)	173(2)	293(2)	293(2)	293(2)
cryst syst	monoclinic	monoclinic	monoclinic	monoclinic	monoclinic	monoclinic	monoclinic
space group	$P2_1/c$	$P2_1/c$	$P2_1/c$	$P2_1/c$	$P2_1/c$	$P2_1/c$	$P2_1/c$
a/Å	12.5918(11)	11.230(9)	12.205(6)	12.664(1)	12.765(4)	11.976(6)	12.225(2)
b/Å	7.6860(7)	7.726(6)	7.725(4)	7.611(8)	7.615(2)	7.669(4)	7.629(1)
c/Å	15.915(2)	15.917(1)	15.865(7)	15.889(2)	16.016(5)	15.986(7)	16.105(2)
β/deg	106.532(7)	106.702(1)	105.256(8)	107.358(2)	108.397(6)	107.529(1)	107.100(2)
V/Å^3	1476.6(2)	1322.7(2)	1443.1(1)	1461.7(3)	1477.4(8)	1400.0(1)	1435.6(3)
Z	4	4	4	4	4	4	4
D_{calcd}/g cm^{-3}	1.665	1.588	1.686	1.728	1.709	1.695	1.722
μ/mm^{-1}	1.202	1.311	1.224	1.212	1.199	1.251	1.227
F(000)	760	640	752	784	784	728	760
no. of reflns collected	6540	4662	5272	7124	7429	7398	7947
no. of independent reflns	2888	2585	2781	3139	3089	2972	3044
R_{int}	0.0934	0.1252	0.0720	0.0520	0.0608	0.0565	0.0446
GOF	0.851	0.959	0.966	1.019	1.084	0.125	1.032
$R_1{}^a$ ($I \geq 2\sigma(I)$)	0.589	0.0704	0.0545	0.0564	0. 0915	0.0731	0.0657
$wR_2{}^b$ (all data)	0.1370	0.1997	0.1462	0.1646	0. 2381	0.1599	0.1691

$^a R_1 = \sum||F_o| - |F_c||/\sum|F_o|$. $^b wR_2 = [\sum w(F_o{}^2 - F_c{}^2)^2/\sum w(F_o{}^2)^2]^{1/2}$.

Table 2. Selected Bond Lengths (Å) and Angles (deg) for **1**−**6** and **4h**[a]

		1	
Co(1)−O(3a)	1.981(3)	Co(1)−N(1b)	2.184(4)
Co(1)−O(1)	2.059(3)	Co(1)−O(1w)	2.244(4)
Co(1)−N(2)	2.092(4)	Co(1)−O(2)	2.368(3)
O(3a)−Co(1)−O(1)	104.8(1)	N(2)−Co(1)−O(1w)	87.1(2)
O(3a)−Co(1)−N(2)	104.2(2)	N(1b)−Co(1)−O(1w)	172.8(1)
O(1)−Co(1)−N(2)	146.7(2)	O(3a)−Co(1)−O(2)	163.2(2)
O(3a)−Co(1)−N(1b)	97.2(1)	O(1)−Co(1)−O(2)	58.5(1)
O(1)−Co(1)−N(1b)	92.1(1)	N(2)−Co(1)−O(2)	91.4(2)
N(2)−Co(1)−N(1b)	100.1(2)	N(1b)−Co(1)−O(2)	86.0(1)
O(3a)−Co(1)−O(1w)	81.3(1)	O(1w)−Co(1)−O(2)	93.5(1)
O(1)−Co(1)−O(1w)	81.5(1)		
		2	
Co(1)−O(3a)	1.949(5)	Co(1)−N(1b)	2. 123(7)
Co(1)−O(1)	1.993(5)	Co(1)−O(2)	2. 324(5)
Co(1)−N(2)	2.069(6)		
O(3a)−Co(1)−O(1)	100.8(2)	N(2)−Co(1)−N(1b)	102. 9(2)
O(3a)−Co(1)−N(2)	102.0(2)	O(3a)−Co(1)−O(2)	159.8(2)
O(1)−Co(1)−N(2)	129.6(3)	O(1)−Co(1)−O(2)	60.0(2)
O(3a)−Co(1)−N(1b)	110.9(2)	N(2)−Co(1)−O(2)	87.8(2)
O(1)−Co(1)−N(1b)	109.7(3)	N(1b)−Co(1)−O(2)	83.4(2)
O(1)−Co(1)−O(1w)	82.4(4)		
		3	
Co(1)−O(3a)	1.989(3)	Co(1)−N(1b)	2.192(4)
Co(1)−O(1)	2.071(3)	Co(1)−O(5)	2.251(4)
Co(1)−N(2)	2.094(4)	Co(1)−O(2)	2.345(4)
O(3a)−Co(1)−O(1)	105.3(1)	N(2)−Co(1)−O(5)	89.2(2)
O(3a)−Co(1)−N(2)	103. 6(2)	N(1b)−Co(1)−O(5)	172.0(1)
O(1)−Co(1)−N(2)	147.1(2)	O(3a)−Co(1)−O(2)	164.4(1)
O(3a)−Co(1)−N(1b)	96.5(2)	O(1)−Co(1)−O(2)	59.1(2)
O(1)−Co(1)−N(1b)	93. 1(1)	N(2)−Co(1)−O(2)	91.1(1)
N(2)−Co(1)−N(1b)	98.9(2)	N(1b)−Co(1)−O(2)	86.2(1)
O(3a)−Co(1)−O(5)	81.1(1)	O(5)−Co(1)−O(2)	94.2(1)
O(1)−Co(1)−O(5)	80.2(1)		
		4	
Co(1)−O(3a)	1.966(3)	Co(1)−N(1b)	2. 157(4)
Co(1)−O(1)	2.037(3)	Co(1)−O(5)	2.301(4)
Co(1)−N(2)	2.081(4)	Co(1)−O(2)	2.379(4)
O(3a)−Co(1)−O(1)	103.5(1)	N(2)−Co(1)−O(5)	87.2(2)
O(3a)−Co(1)−N(2)	106.0(2)	N(1b)−Co(1)−O(5)	171.7(2)

Table 2. Continued

	4		
O(1)−Co(1)−N(2)	145.1(2)	O(3a)−Co(1)−O(2)	162.0(1)
O(3a)−Co(1)−N(1b)	94.2(1)	O(1)−Co(1)−O(2)	58.6(2)
O(1)−Co(1)−N(1b)	94.3(2)	N(2)−Co(1)−O(2)	91.3(1)
N(2)−Co(1)−N(1b)	100.6(2)	N(1b)−Co(1)−O(2)	84.9(1)
O(3a)−Co(1)−O(5)	78.6(2)	O(5)−Co(1)−O(2)	97.8(1)
O(1)−Co(1)−O(5)	80.6(2)		
	4h		
Co(1)−O(3a)	1.944(5)	Co(1)−N(1b)	2.158(7)
Co(1)−O(1)	2.106(5)	Co(1)−O(2)	2.402(6)
Co(1)−N(2)	2.079(5)		
O(3a)−Co(1)−O(1)	102.3(3)	N(2)−Co(1)−N(1b)	102.4(2)
O(3a)−Co(1)−N(2)	106.1(2)	O(3a)−Co(1)−O(2)	160.6(2)
O(1)−Co(1)−N(2)	140.6(2)	O(1)−Co(1)−O(2)	58.3(2)
O(3a)−Co(1)−N(1b)	102.0(3)	N(2)−Co(1)−O(2)	90.4(2)
O(1)−Co(1)−N(1b)	97.6(3)	N(1b)−Co(1)−O(2)	83.9(3)
	5		
Co(1)−O(3a)	1.952(4)	Co(1)−N(1b)	2.135(5)
Co(1)−O(1)	2.016(4)	Co(1)−O(2)	2. 370(4)
Co(1)−N(2)	2.057(4)		
O(3a)−Co(1)−O(1)	101.2(1)	N(2)−Co(1)−N(1b)	103.0(2)
O(3a)−Co(1)−N(2)	105.5(2)	O(3a)−Co(1)−O(2)	160.1(1)
O(1)−Co(1)−N(2)	134.4(2)	O(1)−Co(1)−O(2)	59.2(1)
O(3a)−Co(1)−N(1b)	106.6(2)	N(2)−Co(1)−O(2)	88.6(2)
O(1)−Co(1)−N(1b)	103.8(2)	N(1b)−Co(1)−O(2)	83.1(2)
	6		
Co(1)−O(3a)	1.966(4)	Co(1)−N(1b)	2.140(5)
Co(1)−O(1)	2.018(4)	Co(1)−O(2)	2.389(4)
Co(1)−N(2)	2.068(4)		
O(3a)−Co(1)−O(1)	106.1(1)	N(2)−Co(1)−N(1b)	100.5(1)
O(3a)−Co(1)−N(2)	104.7(2)	O(3a)−Co(1)−O(2)	159. 8(1)
O(1)−Co(1)−N(2)	139.2(2)	O(1)−Co(1)−O(2)	58.8(2)
O(3a)−Co(1)−N(1b)	106.6(2)	N(2)−Co(1)−O(2)	89.3(1)
O(1)−Co(1)−N(1b)	100.0(2)	N(1b)−Co(1)−O(2)	82.7(2)

[a] Symmetry codes for **1**−**5**, **4h**: (a) x, $-y + 1/2$, $z + 1/2$; (b) x, $y + 1$, z. Symmetry codes for **6**: (a) x, $-y + 3/2$, $z - 1/2$; (b) x, $y + 1$, z.

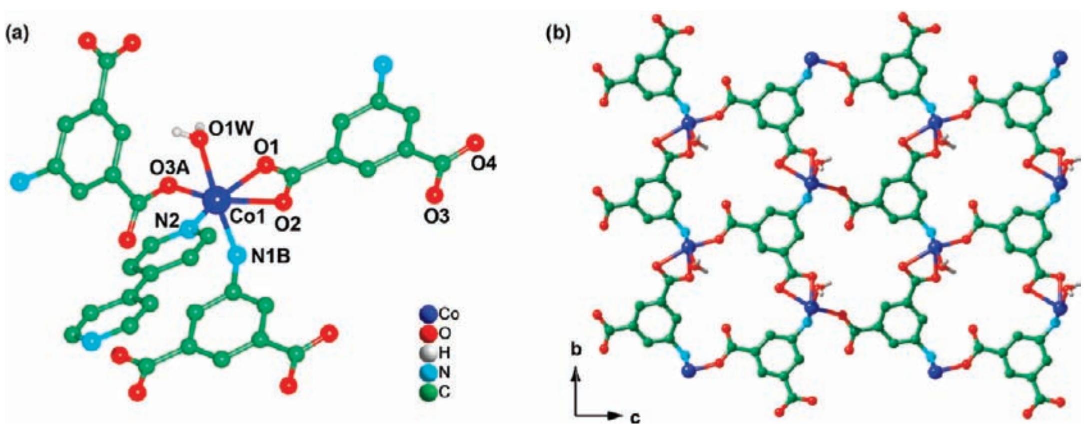

Figure 1. (a) Perspective views of the coordination geometries of Co(II) in **1** (some equivalent atoms have been generated to complete the Co coordination). (b) Perspective views of the 2D $[Co(5\text{-}NH_2\text{-}bdc)(H_2O)]_n$ layer in **1** (most H atoms are omitted for clarity).

An analysis with PLATON[16] suggests that the channels occupy 16.8% of the total volume. Furthermore, the bilayers are closely packed by fitting the grooves together and interconnected by hydrogen bonding between the amino groups and the carboxylate O atoms [N···O = 3.021−3.125 Å]. The thickness of the bilayer is 11.31(1) Å, and the interspaces between adjacent 2D bilayers are less than 0.5 Å, assuming van der Waals radii. Therefore, only the translational motion of guest molecules along the 1D channels inside the pillared bilayer is permissible, as shown in Figure 2b. The pillaring bpy ligands are responsible for

(16) Spek, A. L. *PLATON*; Utrecht University: Utrecht, The Netherlands, 2009.

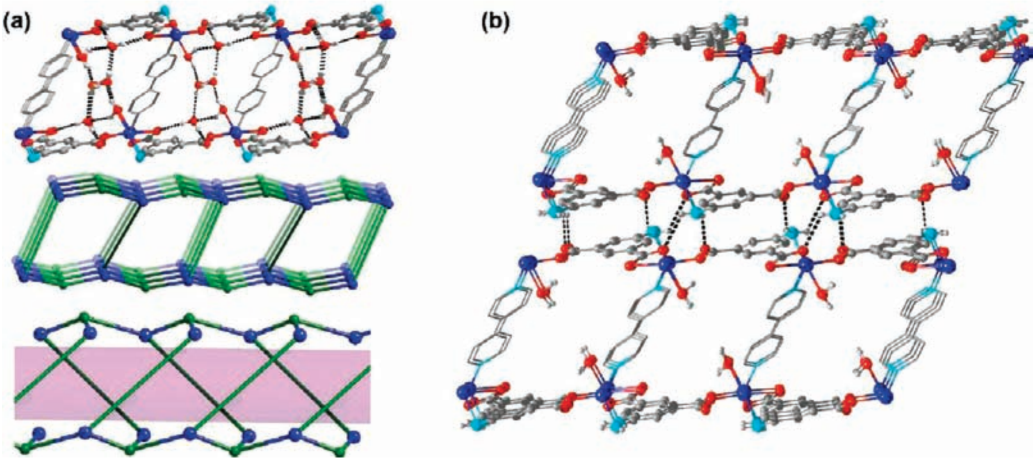

Figure 2. (a) A view of **1** on the *ac* plane showing weak hydrogen bonding in the pillared bilayer (top), highlighting the channels by using a gray color for carbon ions (most H atoms omitted for clarity). Hereafter, the channels motif uses the same color scheme. Schematic presentation showing the 2D structure of **1** (middle), noting the 1D channels apparent (bottom). (b) A view of hydrogen bonding between the 2D layers in **1**.

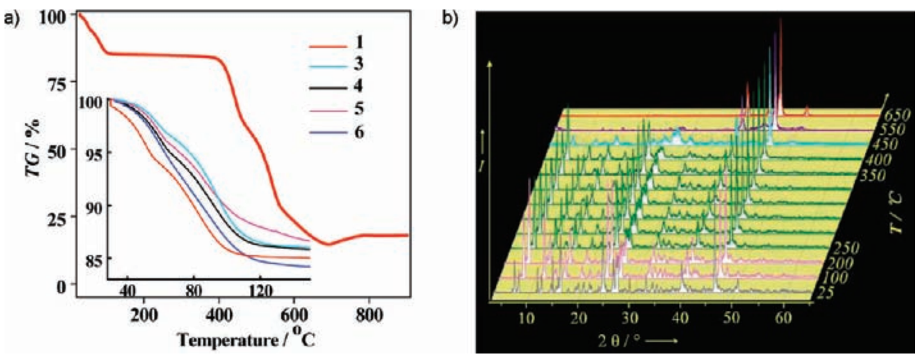

Figure 3. (a) TG curves for as-synthesized and SCSC samples **1**−**6** under a nitrogen atmosphere. (b) Powder XRD pattern of **1** at 25−650 °C.

controlling the overall pillared-layer structures, where the probable rotation of pyridyl groups of bpy along the central C−C bond implies that the large guest incorporated inside the crystal can diffuse through the expandable window of the channel and is fettered in the cavities. The network topology can be simplified by considering just the four-connected Co(II) atom nodes and three-connected 5-NH_2-bdc ligands, as well as the bidentate bpy ligands, as linkers between the Co(II) nodes. The resulting net is a rare 2D (3,4)-connected net with triangular and tetrahedral nodes in a 1:1 ratio (Figure 2b and Figure S1, Supporting Information). A topological analysis of this net was performed with the OLEX program.[17] The long topological (O'Keeffe) vertex symbol is ($6_1 6_1 6_1 6_1 6_1 8_2$) for the four-connected Co(II) node and ($6_1 6_1 6_2$) for the three-connected 5-NH_2-bdc node, giving the short vertex symbol (6^3)(6^5.8). The net is different from other previously identified (3,4)-connected networks[18] and, thus, is unprecedented in coordination networks. Indeed, this compound represents a novel example, which is rarely observed in the mixed, rigidly symmetrical bridging ligands, involving structural diversity and a topology upgrade from a thin layer to a pillared bilayer framework.[3,19]

Thermal Stability. To examine the thermal stability and capacity of the porous pillared bilayer framework, TG analyses and XRPD measurements were carried out (Figure 3). The TG curve of **1** shows that the weight losses of the guest and coordinated water molecules are not resolved, and the experimental mass loss of the steps of about 14.5% indicates the release of all water molecules up to ~113 °C, to give the dehydrated form **2** (calcd, 14.6%). The dehydrated phase remains stable up to 400 °C until the organic ligands start to be released exhibits the high framework stability of **2**. Figure 3b shows the XRPD patterns of the as-synthesized **1** in the range 25−650 °C. It is clear that the diffraction profiles below 400 °C are almost the same, indicating that the microporous framework is stable at this temperature and the crystal lattice remains intact after removal of the guest water molecules. The XRPD pattern recorded at 450 °C exhibits a notable decrease in intensity, but all peaks still match with the simulated one, suggesting that the porous framework is basically maintained. However, the sample became amorphous when the temperature was increased to 550 °C, as shown by the absence of diffraction peaks in

(17) Dolomanov, O. V.; Blake, A. J.; Champness, N. R.; Schröder, M. *J. Appl. Crystallogr*. **2003**, *36*, 1283.

(18) (a) Abrahams, B. F.; Batten, S. R.; Hamit, H.; Hoskins, B. F.; Robson, R. *Angew. Chem., Int. Ed.* **1996**, *35*, 1690. (b) Blatov, V. A.; Carlucci, L.; Ciani, G.; Proserpio, D. M. *CrystEngComm* **2004**, *6*, 377.

(19) (a) Maji, T. K.; Mostafa, G.; Matsuda, R.; Kitagawa, S. *J. Am. Chem. Soc*. **2005**, *127*, 17152. (b) Choi, H. J.; Suh, M. P. *J. Am. Chem. Soc*. **2004**, *126*, 15844.

the XRPD pattern. It can be concluded that **1** has excellent thermal stability.[20,21] The high stability of **1** may also be attributed to the limitedly small porosity, the presence of abundant coordination bonds of the μ_3-bridging modes for 5-NH_2-bdc ligands, and the potently flexible effect of pillared bpy groups between the bilayers.[20]

Single-Crystal-to-Single-Crystal Guest Exchange. De-/Rehydration Transformations of 1−2−1′. The openness of the channels makes it possible to remove the guest and coordinated water molecules from **1**. When crystals of **1** were heated at 120 °C under a vacuum for 2 h to remove the coordinated and guest water molecules, the dehydrated solid [Co(5-NH_2-bdc)$(bpy)_{0.5}$] (**2**) was obtained with retention of the single crystallinity. The crystal structure of **2** confirms that the framework structure and packing mode of **1** is retained and the space previously occupied by water molecules becomes devoid of any appreciable electron density (Figure 4a). Although the crystal system and space group remain unchanged, a molecular rearrangement involving a coordination geometry alteration of Co1 in **2** occurs. The coordination geometry of Co1 changes from an octahedron to a distorted square pyramid. In particular, the O1−Co1−N2 angle decreases from 146.7(2) to 129.7(2)°, and the bond length of Co1−N2 decreases from 2.092(4) to 2.067(6) Å. Accompanying the change in the Co(II) coordination environment, there is a color change from pink to brown (Scheme 1a). The void volume (V_{void}) occupies 16.1% of the total crystal volume for **2**, with effective windows of the channels along the *b* axis being 1.8×5.0 Å^2, which is smaller than that in **1** (3.2×6.2 Å^2). More importantly, the unit-cell volume is decreased from 1476.6(2) to 1322.7(2) Å^3 (Scheme 1b), thus indicating that **2** shrinks in comparison to **1**. In addition, the absence of guest water molecules may initiate a more substantial channel contraction. In contrast, the interlayer distance in **2** decreases from 11.31 to 10.24 Å upon the removal of all water molecules. Instead of simply generating vacant coordination sites, the MOF transforms its geometry to a more thermodynamically stable one. This shrinkage is derived from the cleavage of the apical, long Co−O_{water} bond and the subsequent shear motion of bpy pillars to bring the channel walls closer (Figure 4b). Similar to **1**, weak interlayer N−H···O hydrogen-bonding interactions [N···O = 2.966−3.345 Å] play a vital role in the consolidation of the solid structure. Interestingly, removal of the coordinated water ligands opens new small channels with effective dimensions of 1.7×3.1 Å^2 along the *c* axis. Furthermore, the dehydrated process can be reversed by exposing the dehydrated sample to water vapor for several days or a brief immersion of **2** into water at room temperature. A crystallographic investigation demonstrates that the framework structure of rehydrated **1′** is the same as that of **1**, accompanied by a return of the original color. Thus, in the rehydration process,

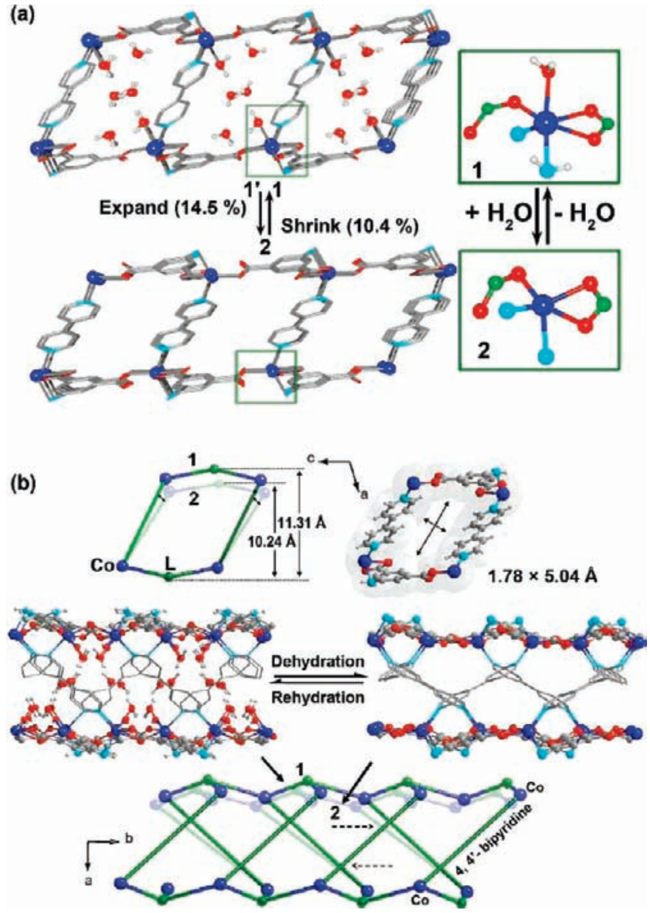

Figure 4. (a) Summary of framework **1** exhibiting reversible single-crystal-to-single-crystal transformation upon removal and rebinding of coordinating water molecules, accompanying a change in the Co(II) coordination environment. Most H atoms are omitted for clarity. (b) A detailed framework of **1** exhibiting spongelike dynamic behavior.

Co1 of **2** provides a coordination site for the water molecule and rearranges to the octahedral coordination geometry. In addition, the bpy pillars undergo reverse shear motion with respect to the cobalt carboxylate planes. In short, the single-crystal transformations of **1** → **2** → **1′** involve dynamic motions altering the coordination geometry of Co(II) from/to an octahedron to/from a square pyramid as well as the shrinkage/expansion of pore deformation.[3-6]

Apical Ligand Substitutions of 1, 3, 4, and 1″. Enlightened by the successful immobilization of UMCs onto the MOF pore and the stability and flexibility of **1** and **2**, we performed crystallographic studies of reversible apical-ligand substitution at the Co(II) center. When the single crystals of **1** were soaked for one day in methanol or ethanol at room temperature, they turned correspondingly into [Co(5-NH_2-bdc)$(bpy)_{0.5}$(MeOH)]·H_2O (**3**) or [Co(5-NH_2-bdc)$(bpy)_{0.5}$(EtOH)]·H_2O (**4**). The crystallographic data of **3** and **4** were collected at 173 K, and those of **3h** and **4h** were collected at 293 K. Although alcohols are very weak ligands, the crystallographic analysis reveals that the apical water molecules are substituted by MeOH (Figure 5) or EtOH (Figure 6) and one guest water molecule per formula unit extruded from the crystal, and one water molecule is still retained in the channel. During the transformation of **1** into **3** or **4**, no significant change

(20) (a) Pan, L.; Parker, B.; Huang, X.-Y.; Olson, D. H.; Lee, J. Y.; Li, J. *J. Am. Chem. Soc.* **2006**, *128*, 4180. (b) Pan, L.; Sander, M. B.; Huang, X.-Y.; Li, J.; Smith, M.; Bittner, E.; Bockrath, B.; Johnson, J. K. *J. Am. Chem. Soc.* **2004**, *126*, 1308.

(21) (a) Zeng, M.-H.; Zhang, W.-X.; Sun, X.-Z.; Chen, X.-M. *Angew. Chem., Int. Ed.* **2005**, *44*, 3079. (b) Zeng, M.-H.; Wang, B.; Wang, X.-Y.; Zhang, W.-X.; Chen, X.-M.; Gao, S. *Inorg. Chem.* **2006**, *45*, 7069.

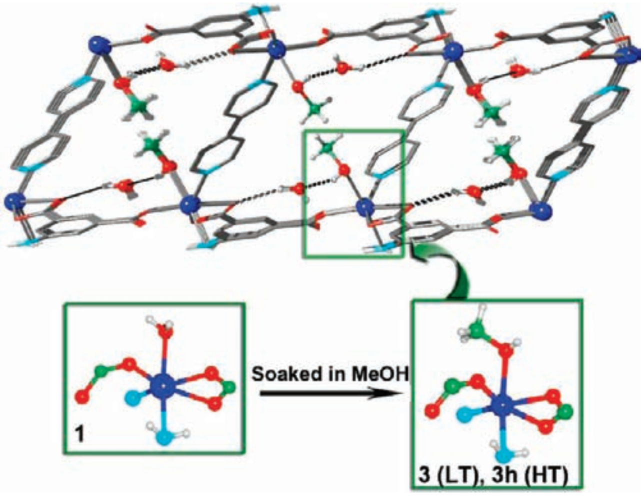

Figure 5. A view of framework **1** exhibiting ligand-exchange behavior in MeOH. Most H atoms are omitted for clarity.

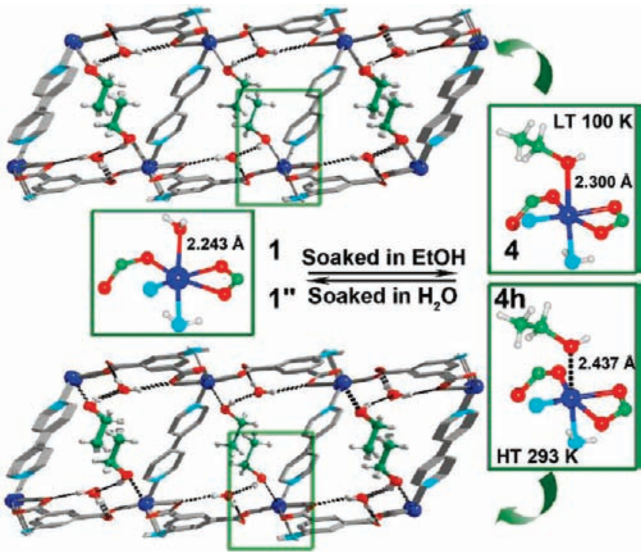

Figure 6. Summary of framework **1** exhibiting reversible ligand-exchange ability in EtOH. Most H atoms are omitted for clarity.

was observed in the unit-cell parameters or the window size of the 1D channel from that of its parent host lattice. It is worth noting that the coordination geometry of **4h** is rather unusual at room temperature. The apical coordinated EtOH molecules are elongated ($Co\cdots O_{EtOH}$ = 2.446 Å). Such a cobalt−oxygen distance is considerably long, beyond the range of classical coordination interaction. This fact implies that the weak-coordination EtOH molecules are easily extruded from the crystal. As expected, the apical-ligand exchange process can be reversed by immersing **4** into water at room temperature, furnishing the initial aqua form (**1**$''$). Obviously, although alcohols are extremely weak ligands, they are able to substitute coordinated water molecules under circumstances of a highly concentrated organic solvent and vice versa. The color of the crystals returned from deep magenta to pink within a few hours. Obviously, the optical observation represents convenient methods for monitoring the chemical change occurring within such crystals.[22,23]

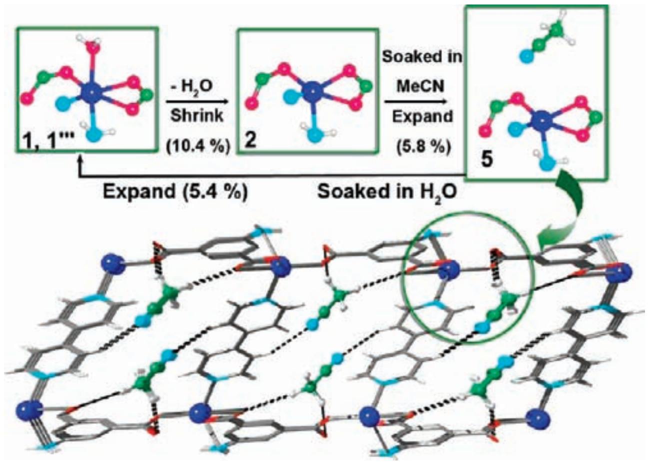

Figure 7. Summary of the MeCN inclusion and exclusion processes of framework **1**. Most H atoms are omitted for clarity.

Guest Inclusion and Shape Recognition of 2, 5, and 6. A detailed analysis of the 1D channel of **2** allows us to speculate that a linear guest molecule may fit the rectangular pore efficiently and undergo a shape recognition transformation. Crystalline samples of dehydrated phase **2** were immersed in acetonitrile or 2-propynyl alcohol; they turned into $[Co(5\text{-}NH_2\text{-bdc})(bpy)_{0.5}]\cdot MeCN$ (**5**) or $[Co(5\text{-}NH_2\text{-bdc})(bpy)_{0.5}(PPA)_{0.5}]\cdot(PPA)_{0.5}$ (**6**, PPA = propynyl alcohol), followed by a corresponding expansion of the "soft" supramolecular framework. Although **2** exhibits vacant coordination sites, the extremely weak-coordination MeCN molecules are not contacted by the unsaturated cobalt centers, merely diffusing into the expandable windows of the channels. Only nonclassical weak $C-H\cdots O/C-H\cdots N$ hydrogen-bonding interactions are present between the methyl hydrogen atoms/CN group of the erect MeCN and oxygen atoms of the L/C−H groups of bpy on the host framework ($C\cdots O$ = 3.37−3.42 Å/$C\cdots N$ = 3.42 Å) (Figure 7). Some marked difference in the MeCN and PPA guest inclusion was observed. From further analysis of the structure of **6**, three unique features are apparent: (1) The structure of the PPA molecule shows roughly 50% positional disorder in head-to-tail fashion. (2) A total of 50% of PPA is weakly coordinated to unsaturated cobalt(II) centers ($Co\cdots O$ = 2.453 Å), altering the coordination geometry of Co(II) from square pyramid to octahedron; 50% of UMCs remain unchanged. (3) The pore volume is totally occupied by the long-chain PPA molecules. The pillared bilayer framework undergoes an expansive deformation such that the channel cavities suit the rigid PPA molecules very well (Figure 8). A significant $O-H\cdots O$ hydrogen-bonding interaction [$O\cdots O$ = 2.745−2.746 Å] between the alcohol group of PPA and the oxygen atom of the coordinated carboxylate of 5-NH_2-bdc plays a vital role

(22) (a) Neville, S. M.; Halder, G. J.; Chapman, K. W.; Duriska, M. B.; Southon, P. D.; Cashion, J. D.; Letard, J.-F.; Moubaraki, B.; Murray, K. S.; Kepert, C. J. *J. Am. Chem. Soc.* **2008**, *130*, 2869. (b) Supriya, S.; Das, S. K. *J. Am. Chem. Soc.* **2007**, *129*, 3464. (c) Suh, M. P.; Cheon, Y. E.; Lee, E. Y. *Chem.—Eur. J.* **2007**, *13*, 4208. (d) Wu, C.-D.; Lin, W.-B. *Angew. Chem., Int. Ed.* **2005**, *44*, 1958. (e) Cussen, E. J.; Claridge, J. B.; Rosseinsky, M. J.; Kepert, C. J. *J. Am. Chem. Soc.* **2002**, *124*, 9574.

(23) Bradshaw, D.; Warren, J. E.; Rosseinsky, M. J. *Science* **2007**, *315*, 977.

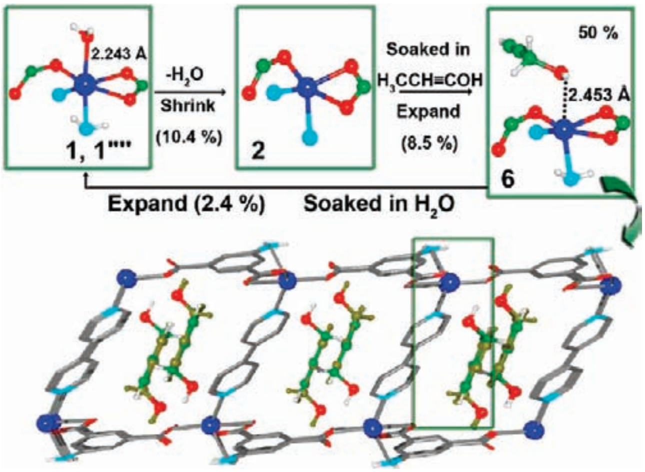

Figure 8. Summary of the 2-propynyl alcohol inclusion and exclusion processes of framework **1**. Most H atoms are omitted for clarity.

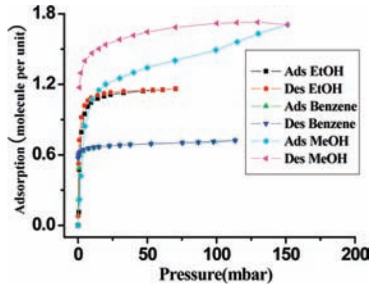

Figure 9. Adsorption and desorption isotherms for different adsorbates in **2** at 298 K: MeOH, EtOH, and benzene.

in the consolidation of the host−guest system. Interestingly, these crystals of dynamic guest inclusions are reversible. When the crystals of **5** or **6** were immersed in water for 2 h, rehydrated crystal **1'''**/**1''''** resulted. The X-ray crystal structure of **1'''**/**1''''** indicates that the original structure of **1** is restored with dominant water molecules intrusion, even though large guests were embedded in the pore. Retention of the single crystallinity upon this guest-inclusion process must be attributed to the existence of 1D channels in the flexibile framework and effective shear motion of pillars, which offer no stress to the crystals during the guest-exchange processes.[4,24]

Sorption Properties. The well-defined structural changes upon SCSC transformation of the flexible porous framework allow us to make a good system for adsorption. Expansion of the host framework of **2** is feasible, corresponding to the foregoing SCSC transformation studies, so that samples of [Co(5-NH_2-bdc)(bpy)$_{0.5}$] were subjected to vapor adsorption measurements using oversized MeOH, EtOH, and benzene molecules (Figure 9). A rapid increase in the amount of adsorbed vapor is shown by an increase under low pressure, which indicates the diffusion of adsorbates into the channels. Approximately 1.7 MeOH, 1.2 EtOH, and 0.7 benzene molecules were adsorbed per formula unit at a pressure of 151.1, 70.5, and 113.4 mbar, respectively, despite their diameter (> 3.0 Å) being greater than the narrowest part (1.8 Å) of the rectangular window of **2**. There are apparent structural changes that can be evaluated from the isotherms. There should be a dynamic expansion of the host framework when large guest molecules diffuse into the small cavities, giving a new undefined solid phase, whose windows should be expanded not only to be greater than the size of benzene (3.3 × 6.6 Å^2) but also to be greater than the original pore size of **1** (3.2 × 6.2 Å^2). Moreover, adsorption and desorption experiments with EtOH or benzene trace the same isotherms, respectively, which indicate that the channel structures are retained through those processes. The desorption curve of MeOH does not coincide with the adsorption one, showing large hysteresis and inapparent desorption, which suggest that MeOH molecules are fettered in each cavity. This characteristic desorption profile also agrees with the results of crystallographic analyses for foregoing SCSC transformation, with some of the MeOH molecules, which have better coordinating ability than EtOH molecules, chemically binding to the coordinatively unsaturated Co(II) centers.[25,26] The porosity of **2** was further examined by gas sorption measurements. The adsorption isotherm of N_2 (Figure S2, Supporting Information, at 77 K) shows that only surface adsorption has occurred, indicating that nitrogen molecules cannot diffuse into the channels at this temperature. This phenomena can be attributed to the presence of the narrow pore size (1.8 × 5.0 Å^2) of **2**, which does not permit N_2 (3.64 Å) to access the channels. Obviously, the N_2 gas is different with the organic vapor and has no ability to bend or rotate molecular linkages enough to a gate opening at 77 K under low pressure.[24]

TG Analyses and Molar Enthalpies of Crystalline State−Liquid Ligand Substitution and Guest Exchange/Inclusion in 1 and 2. TG analyses of crystalline samples of **1** after the exchange of guest or coordinating molecules from different solutions of MeOH (**3**), EtOH (**4**), MeCN (**5**), and PPA (**6**) show the release of guest and coordinated molecules in different steps (Figure 3a). The guest water and coordinated molecules, the weight loss observed (%), and the temperature (°C) are as follows: MeOH and H_2O, 13.3, ∼125; EtOH and H_2O, 14.6, ∼160; MeCN, 12.0, ∼127; PPA, 14.7, ∼141. The results agree with the crystallographic analyses, which confirm the capacity of the pillared bilayer framework for the capture of variform molecules. On the other hand, the molar enthalpies of crystalline state−liquid guest exchange and guest inclusion processes in **1** and **2** using the microcalorimetric method have been studied (Scheme 2). The small value and positive signs of the molar enthalpy ΔH_m^θ (from +12.68 to +25.92 kJ/mol) indicate that the crystalline state−liquid reactions are endothermic. During the apical-ligand exchange processes of hydrated phase **1**, the values of the molar enthalpy of **1** ⊃ MeOH (21.38 ± 0.96 kJ mol^{-1}) and **1** ⊃ EtOH (12.68 ± 0.85 kJ mol^{-1}) are less than those of the guest inclusion process of dehydrated phase **2** (**2** ⊃ MeOH, 25.92 ± 0.86 kJ mol^{-1}; **2** ⊃ EtOH, 17.03 ± 0.57 kJ mol^{-1}), by values of 4.54 and 4.35 kJ mol^{-1}. The value in the **2** ⊃ MeCN process is 14.93 ± 0.75 kJ mol^{-1}. The apparent energy of the reactions indicates that crystalline-state guest exchange and guest inclusion in SCSC

(24) Kubota, Y.; Takata, M.; Kobayashi, T. C.; Kitagawa, S. *Coord. Chem. Rev.* **2007**, *251*, 2510.
(25) (a) Zhang, J.-P.; Kitagawa, S. *J. Am. Chem. Soc.* **2008**, *130*, 907. (b) Zhang, J.-P.; Horike, S.; Kitagawa, S. *Angew. Chem., Int. Ed.* **2007**, *46*, 889.
(26) Zhang, J.-P.; Chen, X.-M. *J. Am. Chem. Soc.* **2008**, *130*, 6010. (b) Zhang, J.-P.; Chen, X.-M. *J. Am. Chem. Soc.* **2009**, *131*, 5516.

processes is a spontaneous endothermic reaction and can be feasibly tracked using the microcalorimetric method. According the above results, along with the static structure determination, it is noted that the needed energy to bend or rotate host molecular linkages and separate the solvent molecules from the liquid phase by breaking weak interactions is obviously larger than the energies contributed from host−guest interaction. On the other hand, the energies contributed by the interaction from water molecules diluting into the solvent is more dominating than that of the weak coordination interaction from apical-ligand substitution.[26,1f] In other words, the above processes are entropy-driving reactions. In fact, in the multi-interaction crystalline state−liquid reaction processes, the molar enthalpy results from the cooperative effect for apical coordinating substitution, bending and rotation of the molecular linkages, and breakage of weak intraframework interactions, as well as the various formation or breakage of the weak interaction among solvent molecules in the liquid phase and so forth.[3−6] Although it is not easy to understand the SCSC reaction solely on the basis of the thermochemistry cycle, all gained parameters of molar enthalpy would offer essential technical parameters for application of the title complex. The main difficulty in the method is to prepare the single crystals with uniform size, which sensitively exhibit different surface interactions in the solid−liquid heterogeneous system and the complex weak interaction when the guest diffuses into the solvent and solvent molecules diffuse into the microspace. In this work, a simple new method for the measurement of molar enthalpies of crystalline state−liquid ligand substitution and guest exchange/inclusion is developed. Further investigations, employing improved techniques, are required to delineate detailed SCSC transformation−energy relationships for these systems.

Conclusions

This work exhibits a series of interesting spongelike dynamic behaviors triggered by removing and rebinding of the coordinated molecules or by oversized guest molecules' intrusion into a Co(II)-based flexible 2D pillared-bilayer porous framework demonstrated by complete X-ray single-crystal analyses. It is also a novel example in MOFs with coordinatively unsaturated metal centers undergoing a shape recognition process for different organic solvents upon SCSC transformations. The vapor adsorptions of dehydrated forms also demonstrate that oversized guest molecules can be incorporated into the channels depending on the framework expansion and gate-opening phenomenon. Furthermore, we note that the microcalorimetric method gives an opportunity to observe and characterize structural and chemical change during crystalline state−liquid reactions, besides a range of different single-crystal techniques. Finally, our results provide a hint for the design of a "soft" 3D framework with a 2D pillared bilayer motif consolidated by supramolecular interactions.

Acknowledgment. This work was supported by NSFC (No. 20561001), SFGX (No. 0832001Z), the Program for New Century Excellent Talents in University of the Ministry of Education China (NCET-07-217), and the Project of Ten, Hundred, Thousand Distinguished Talents in New Century of Guangxi (No. 2006201) as well as GKN (Grant 0630006-5D).

Supporting Information Available: X-ray crystallographic files for **1**−**6** and **4h** (CIF) as well as additional figures and tables. This material is available free of charge via the Internet at http://pubs.acs.org.